Made available through Montana State University's ScholarWorks

Active conversion of atmospheric carbon dioxide to methane in peridotites of the Samail Ophiolite, Oman

Daniel B. Nothaft; Alexis S. Templeton; Peter B. Kelemen; Eric S. Boyd; Juerg M. Matte

Accessibility Disclaimer:

For a more accessible version of this document, please submit an accessibility request form through the Montana State University Library website.

scientific reports

Check for updates

OPEN

Active conversion of atmospheric carbon dioxide to methane in peridotites of the Samail Ophiolite, Oman

Daniel B. Nothaft[1,5]✉, Alexis S. Templeton[1]✉, Peter B. Kelemen[2], Eric S. Boyd[3] & Juerg M. Matter[4]

Methane (CH_4) is common in fluids sourced from low-temperature hydrating (serpentinizing) peridotites, but the carbon sources, rates, and mechanisms of CH_4 formation are uncertain. In CH_4 dissolved in groundwaters pumped from four wells of up to 400 m depth in the Samail Ophiolite, Oman, we observed ^{14}C contents ranging from radiocarbon-dead to 0.3038 ± 0.0015 fraction modern. Chemical and isotopic analyses of groundwaters and hydrocarbon gases align with microbiological data indicating that methanogens inhabiting H_2-rich ($> 100 \mu mol L^{-1}$), $pH > 11$ fluids produce the ^{14}C-rich CH_4. This "young" microbial CH_4 constitutes a portion of the light hydrocarbons dissolved in the subsurface fluids, which also contain a distinct pool of relatively ^{13}C- and ^{2}H-enriched CH_4 and C_{2+} alkanes that are likely abiotic and older. Our study of groundwaters accessed via wells complements prior studies, which have mostly found ^{14}C-free, gas-phase CH_4 from natural seeps in ophiolites and interpreted an abiotic source from unsaturated rocks. Most importantly, our radiocarbon data show that transport and localized conversion of atmospheric CO_2 to CH_4 in peridotites reacting with water at temperatures < 60 °C occurs at surprisingly fast rates, within the last 10 000 years.

The system carbon–oxygen-hydrogen (C-O–H) within exposures of ultramafic rock as found in ophiolites has broad relevance to volatile exchange with the atmosphere, subsurface microbiology, and the potential for engineered acceleration of fluid-rock reactions including economic production of geologic hydrogen (H_2) and carbon mineralization [1–3]. At temperatures $< 400°C$ and pressures < 100 MPa, ultramafic rocks such as peridotite hydrate and oxidize (serpentinize), forming variable amounts of serpentine, magnetite, brucite, H_2, and other phases, which can coexist with alkaline (pH 8 to 9) and hyperalkaline (pH 10 to 13) aqueous fluids[4]. Where serpentinization occurs under reduced, low fluid-rock ratio conditions, methane (CH_4) is thermodynamically predicted to be the predominant carbon species in the fluids[4,5]. However, laboratory experiments have found strong kinetic inhibitions to the abiotic reduction of aqueous inorganic carbon to CH_4[6]. In contrast, experiments with CO_2 and H_2 in gas phase have produced CH_4 over a wide range of temperatures, down to 25 °C in the presence of metal-bearing catalysts, especially those containing ruthenium, which is found in accessory minerals associated with chromite in ophiolites[6–12]. Another known CH_4 production route involves fluid inclusions formed in the ocean crust and mantle lithosphere that create closed-system conditions wherein gas-phase CO_2 and H_2 can form and interact with surfaces within crystals, mostly at temperatures > 200 °C[13–16]. CH_4-bearing fluids in these inclusions can be stored over millions of years and later released through decrepitation at lower temperatures.

Globally, most CH_4 ^{14}C measurements from serpentinization settings have had minor or no detectable ^{14}C. In all of five ^{14}C analyses of CH_4 from ophiolites in Spain, Turkey, Italy, and the Philippines[17–20], ^{14}C contents have been below detection limits ($F^{14}C$ typically < 0.002, practically radiocarbon-dead). Four of four CH_4 ^{14}C analyses on samples from wells in the Hakuba Happo continental serpentinite in Japan had low but statistically non-zero $F^{14}C$ values ranging from 0.0017 ± 0.0002 to 0.0065 ± 0.0002[21]. One of one CH_4 sample from the ophiolite-hosted Bulqizë chromite mine in Albania had $F^{14}C$ of 0.0376 ± 0.0006[22]. Three of three CH_4 samples from the Prony Bay

[1]Department of Geological Sciences, University of Colorado, Boulder, CO, USA. [2]Lamont-Doherty Earth Observatory, Columbia University, Palisades, NY, USA. [3]Department of Microbiology & Cell Biology, Montana State University, Bozeman, MT, USA. [4]National Oceanography Centre Southampton, University of Southampton Waterfront Campus, Southampton, UK. [5]Present address: Uplift Geosystems LLC, Baltimore, MD, USA. ✉email: daniel.nothaft@colorado.edu; alexis.templeton@colorado.edu

Well	Depth to water /[m]	Pump depth/[m]	Conductivity / [mS cm^{-1}]	Temperature/[°C]	pH	*Eh*/[mV]	$\sum$ Na	$\sum$ Ca	SO_4^{2-}	Cl^-
NSHQ14	8.36	84	2.43	37.1	11.07	−290.	8.92×10^3	4.02×10^3	4.73×10^1	1.45×10^4
NSHQ14[a]	8.39	84	2.84	36.7	11.20	−480.	1.08×10^4	4.09×10^3	5.09	1.62×10^4
WAB71	7.30	79	2.08	34.5	11.09	−339	5.61×10^3	3.82×10^3	5.10×10^1	1.26×10^4

Table 1. Chemical compositions of water samples. Concentrations reported in μmol L^{-1}. Data on an expanded set of analytes are available in the online supplementary materials. Depths referenced to ground level. [a] Well not purged prior to sampling.

Well	H_2	CH_4	C_2H_6	C_3H_8	*i*-C_4H_{10}	*n*-C_4H_{10}	*i*-C_5H_{12}	*n*-C_5H_{12}	C_6H_{12}[a]
NSHQ14	2.45×10^2	7.31×10^1	1.08×10^{-1}	1.27×10^{-2}	$< 4.13 \times 10^{-3}$	$< 5.45 \times 10^{-3}$	$< 3.27 \times 10^{-3}$	4.04×10^{-3}	7.17×10^{-3}
NSHQ14[b]	4.67×10^2	1.28×10^2	2.91×10^{-1}	3.11×10^{-2}	$< 4.13 \times 10^{-3}$	$< 5.45 \times 10^{-3}$	$< 3.27 \times 10^{-3}$	$< 3.63 \times 10^{-3}$	8.34×10^{-3}
WAB71	< 3.29	2.54×10^1	$< 8.63 \times 10^{-3}$	$< 6.81 \times 10^{-3}$	$< 4.13 \times 10^{-3}$	$< 5.45 \times 10^{-3}$	$< 3.27 \times 10^{-3}$	$< 3.63 \times 10^{-3}$	7.13×10^{-3}

Table 2. Aqueous gas concentrations, reported in μmol L^{-1}. [a]Hexane isomers not chromatographically resolved. [b] Well not purged (NP) prior to sampling.

Hydrothermal Field, New Caledonia had detectable ^{14}C, corresponding to ^{14}C ages ranging from 49 500 yr BP to 12 000 yr BP [23]. The Prony Bay Hydrothermal Field consists of meteoric waters that have reacted with ophiolite-hosted peridotites and discharge in a submarine environment. Mixing calculations suggested that 22% microbial CH_4 and 78% abiotic CH_4 could explain the ^{14}C age of 12 000 yr BP [23]. At the Lost City hydrothermal field, which is located in serpentinizing peridotites intermingled with gabbros 15 km from the spreading axis of the Mid-Atlantic Ridge and hosts carbonate-brucite chimneys through which hyperalkaline fluids vent at < 120 °C[24,25], CH_4 is largely ^{14}C-free. Three of six Lost City CH_4 samples were within analytical uncertainty of zero F^{14}C, while the other samples had F^{14}C values of 0.0027 ± 0.0023, 0.0062 ± 0.0054, and 0.0034 ± 0.0011[26]. For comparison, ^{14}C dating of carbonate veins in ophiolites has revealed extensive mineralization of CO_2 on < 50 000-year timescales[1,27]. These data suggest that CH_4 formation occurs at slower rates than CO_2 mineralization during low-temperature peridotite alteration or that CH_4 is largely formed from non-atmospheric C sources.

The Samail Ophiolite of Oman and the United Arab Emirates, where > 20 000 km^3 of peridotite continue to hydrate and carbonate at low temperatures (largely < 60°C)[1,28,29], contains a wide array of wells and springs that enable sampling of fluids representing various geochemical states of the system. Gas molecular and stable isotopic compositions and biomolecular and microcosm data from the Samail Ophiolite are consistent with mixtures of abiotic and microbial CH_4, although their proportions, variability, production rates, and carbon sources are not precisely known[29–36]. To assess the rates and C sources of CH $_4$ production in the fissured rock aquifers in the ophiolite, we determined the ^{14} C content of CH $_4$ via accelerator mass spectrometry on gases exsolved from groundwater samples pumped from wells.

Results

Aqueous geochemistry and stable isotopic compositions of gases

We obtained CH_4 samples for ^{14} C analysis from four wells of up to 400 m depth, which were sampled between 2017 and 2019. The well locations and geologic setting within the mantle section of the ophiolite were previously reported[33]. The CH_4-bearing groundwaters ranged in pH from 10. to 11.39 throughout the sampling period, which is characteristic of extensive reaction with peridotite in near complete isolation from the atmosphere[28,37]. The groundwaters were also strongly reduced ($Eh = -290.$mV, $f_{O_2} = 3.13 \times 10^{-55}$bar to $Eh = -480.$mV, $f_{O_2} = 3.68 \times 10^{-67}$bar in 2019; Table 1), which is typical of hyperalkaline $Ca^{2+} - OH^-$ fluids [34,38].

Concentrations of dissolved H_2 were variable across groundwaters pumped from the wells, with well NSHQ14 having extremely high concentrations (up to 467μmol L^{-1} in 2019), while the other wells including well WAB71 had single-digit μmol L^{-1} concentrations or less (Table 2). Groundwaters sampled from wells in 2019 had high concentrations of dissolved CH_4 (25.4μmol L^{-1} at WAB71 and up to 128μmol L^{-1} at NSHQ14; Table 2). Alkanes of two to six carbons (C_{2+}) were detected, and well NSHQ14 had the highest C_{2+} alkane concentrations (Table 2). The ratios of CH_4 to ethane and propane ($C_1/(C_2 + C_3)$) dissolved in groundwaters from NSHQ14 were 397 to 605 in 2019 (Supplementary Note 1).

The proportions of C_1 through C_6 alkanes from NSQH14 were tested for conformance to the Anderson-Schulz-Flory (ASF) distribution, which is a log-linear relationship of decreasing mole fraction versus increasing C atoms per molecule (C number) that is characteristic of (though not exclusive to) both the synthetic and natural CO_2 or CO hydrogenation to hydrocarbons[39–41]. The alkane proportions in samples from NSHQ14 from 2017, 2018, and 2019 were similar, although samples from 2019 (Table 2) had relatively less (below quantitation) butane and relatively more hexane than in 2017 or 2018[33] (Supplementary Fig. 1). For testing of the ASF distribution, the gas composition from NSHQ14 in 2018 was used because a full suite of C_1 through C_6 alkanes

Well	$\delta^{13}C - CH4$	$\delta^{2}H - CH_4$	$\delta^{13}C - C_2H_6$	$\delta^{13}C - C_3H_8$
NSHQ14	6.5[a],7.2	−263	−5.5	4.9
NSHQ14[b]	4.5	−251	n.d	n.d
WAB71	7.0	−304	n.d	n.d

Table 3. Isotopic compositions of CH_4, C_2H_6, and C_3H_8. All isotopic values reported in ‰ units. $\delta^{13}C$ and $\delta^{2}H$ reported in the VPDB and VSMOW reference frames, respectively. *Abbreviations:* n.d., not determined, [a] Measured by Isotech. [b] Well not purged (NP) prior to sampling.

Well	Year sampled	Pump depth/[m][a]	Accession #[b]	$\delta^{13}C$/[‰ VPDB][c]	Fraction modern ($F^{14}C$)	^{14}C age/[yr BP][d]
NSHQ14	2019	84	OS-152137	n.d	$0.0614 \pm 0.001\,40$	$22\,400 \pm 180$
NSHQ14	2019	84	CURL-26148	0.5	0.0566 ± 0.0006	$23\,070 \pm 90$
NSHQ14[e]	2019	84	CURL-26147	2.5	0.0497 ± 0.0006	$24\,110 \pm 100$
NSHQ14	2018	84	CURL-24538	−3.2	0.3038 ± 0.0015	9570 ± 45
NSHQ14	2017	84	CURL-24539	1.1	0.1918 ± 0.0010	$13\,265 \pm 45$
WAB71	2019	79	CURL-26149	3.2	-0.0001 ± 0.005	$> 42\,600$
WAB71	2018	69	CURL-24537	3.0	-0.002 ± 0.0000	$> 42\,200$
NSHQ04	2018	7	CURL-24535	−0.7	0.0069 ± 0.0010	$39\,950 \pm 1210$
CM2A	2018	74	CURL-24536	−7.0	0.0002 ± 0.0011	$> 48\,100$

Table 4. Radiocarbon measurements. n.d. = not determined. [a]Depths referenced to ground level. [b] "CURL" samples prepared at CU-Boulder and measured at UC-Irvine. "OS" samples prepared at Isotech and measured at NOSAMS. [c]$\delta^{13}C$ value reported here is the AMS measurement, which can be fractionated from the original sample material (typically by 1‰ to 3‰) due to the graphitization process. [d]Conventional age[44,45]. [e]Well not purged prior to sampling.

including isobutane and isopentane were above the limit of quantitation for that sample year (Supplementary Fig. 2). Methane comprised a two to three orders of magnitude higher proportion of NSHQ14 hydrocarbons than the ideal ASF distribution. However, the relationship between $\log_{10}$ (mol fraction) and C number for C_2 to C_6 hydrocarbons was relatively linear ($R^2 = 0.89$), suggesting that polymerization of alkanes larger than methane may be consistent with the ASF distribution. To contextualize NSHQ14 hydrocarbon distributions in relation to another thoroughly studied site of low-temperature serpentinization, low-molecular-weight hydrocarbon concentrations from the Lost City Hydrothermal Field at the Mid-Atlantic Ridge were plotted alongside NSHQ14 (Supplementary Fig. 2). The plotted points represent mean concentrations of the 30 samples reported by Proskurowski et al., who reported concentrations of hydrocarbons up to C number 4[26]. The standard error of the mean of Lost City hydrocarbon concentrations of each respective C number were $< 8\%$ of their mean, indicating low variability in the data set. Overall, the distribution of hydrocarbons at Lost City and NSHQ14 were similar, particularly from C_1 to C_3. The ASF relationship was more linear for Lost City ($R^2 = 0.99$) compared to NSHQ14 in the C_2 through C_4 range ($R^2 = 0.86$).

The carbon stable isotopic compositions of CH_4, C_2H_6, and C_3H_8 in the studied groundwater samples were highly enriched in ^{13}C (−5.5 ‰VPDB to +7.2 ‰VPDB $\delta^{13}C$ in 2019; Table 3; Supplementary Fig. 3) relative to $\delta^{13}C$ values of more widely studied alkane gases in sedimentary reservoirs. Similar ^{13}C enrichment in CH_4 and C_{2+} alkanes has been reported for many serpentinite-hosted sites, including elsewhere in the Samail Ophiolite[2,30,33,42]. The hydrogen stable isotopic compositions of CH_4 measured in our samples (−304 ‰VSMOW to −251 ‰VSMOW $\delta^{2}H$ in 2019; Table 3) fall within the middle range of compositions reported for CH_4 in both sedimentary and serpentinite-hosted settings[33,42].

Supporting data from samples obtained in 2017 and 2018 have been reported previously[32,33]. Thus, we focus the presentation of supporting data here on samples obtained in 2019, when only two wells were sampled for CH_4 ^{14}C, wells NSHQ14 and WAB71. Groundwaters pumped from NSHQ14 at 84 m depth had somewhat variable conservative ion concentrations and pH throughout the study period (pH 11.07 to 11.39). The pH, chemical composition, and gas chemical and isotopic compositions from groundwaters sampled from WAB71 did not vary substantially across the study period. The wells sampled for CH_4 ^{14}C analysis in 2018 only (NSHQ04 and CM2A) were broadly more similar in redox state to WAB71 than NSHQ14 in that they had single-digit μmol H_2 L^{-1} or less in 2018 samples. Additional context on CM2A and NSHQ04 is provided in Supplementary Discussion 1.

Methane radiocarbon data

To determine whether atmospheric CO_2 is converted to CH_4 in fissured rock aquifers within the Samail Ophiolite and potential rates of that conversion, we measured the ^{14}C content of CH_4 exsolved from groundwater samples. Methane from well NSHQ14 had fraction modern ($F^{14}C$) ranging from 0.0497 to 0.304 in samples obtained

in 2017, 2018, and 2019, corresponding to ^{14}C ages of 24.10kyr BP to 9.57 kyr BP (Table 4). The finding of $F^{14}C$ up to 0.304 means that 30 % or more of the CH_4 in that sample was recently (< 10 kyr BP) derived from atmospheric CO_2. In the other well for which CH_4 in groundwater had ^{14}C content significantly above blanks, well NSHQ04, CH_4 $F^{14}C$ was much lower (0.007). In groundwater samples from the two remaining wells, CM2A and WAB71, CH_4 ^{14}C contents were indistinguishable from analytical blanks[43] (radiocarbon dead). This indicates that the CH_4 sampled from those sites was produced from one or more radiocarbon-dead C source(s), was produced > 50 kyr BP, or both. For samples from NSHQ14, negative, linear correlations were found between $\delta^{13}C_{CH_4}$ and $F^{14}C_{CH_4}$ ($R^2 = 0.91, p = 0.01, n = 5$) as well as $\delta^2H_{CH_4}$ and $F^{14}C_{CH_4}$ ($R^2 = 0.88$, $p = 0.06$, $n = 4$) (Fig. 1). Accordingly, $\delta^{13}C_{CH_4}$ and $\delta^2H_{CH_4}$ had a positive, linear correlation ($R^2 = 0.67$, $p = 0.004$, $n = 10$; Supplementary Fig. 4 [33]).

16S rRNA gene sequencing and analysis

To assess the role microbes may play in CH_4 production or consumption in the study area, genomic DNA was extracted from biomass filtered (0.22 µm) from groundwaters and was subjected to PCR amplification and sequencing of 16S rRNA genes. 24% of the 16S rRNA gene sequences in NSHQ14 groundwater communities in 2019 were affiliated with the archaeal genus *Methanobacterium* (Fig. 2), whose members are obligately anaerobic and produce CH_4 from CO_2 using H_2, CO, or formate as electron donor[46]. In contrast, nearly 93% of the 16S rRNA gene sequences in WAB71 communities in 2019 were affiliated with the bacterial class, Thermodesulfovibrionia (Fig. 2). Cultured representatives of Thermodesulfovibrionia are capable of SO_4^{2-} reduction coupled to H_2 oxidation; some strains may additionally/alternatively oxidize C_1-C_3 acids and respire thiosulfate, sulfite, Fe^{3+} or NO_3^- [47,48]. 16S rRNA gene sequences affiliated with *Methanobacterium* were not detected in samples from WAB71. The only other taxon known to produce or consume CH_4 in this data set was affiliated with the genus *Methylococcus* (< 1 % of reads in both NSHQ14 and WAB71 [49]), which contains aerobic methanotrophs [50]. Likewise, groundwater communities in CM2A and NSHQ04 had low relative abundances of 16S rRNA gene sequences affiliated with *Methanobacterium* (<1% of reads [33]).

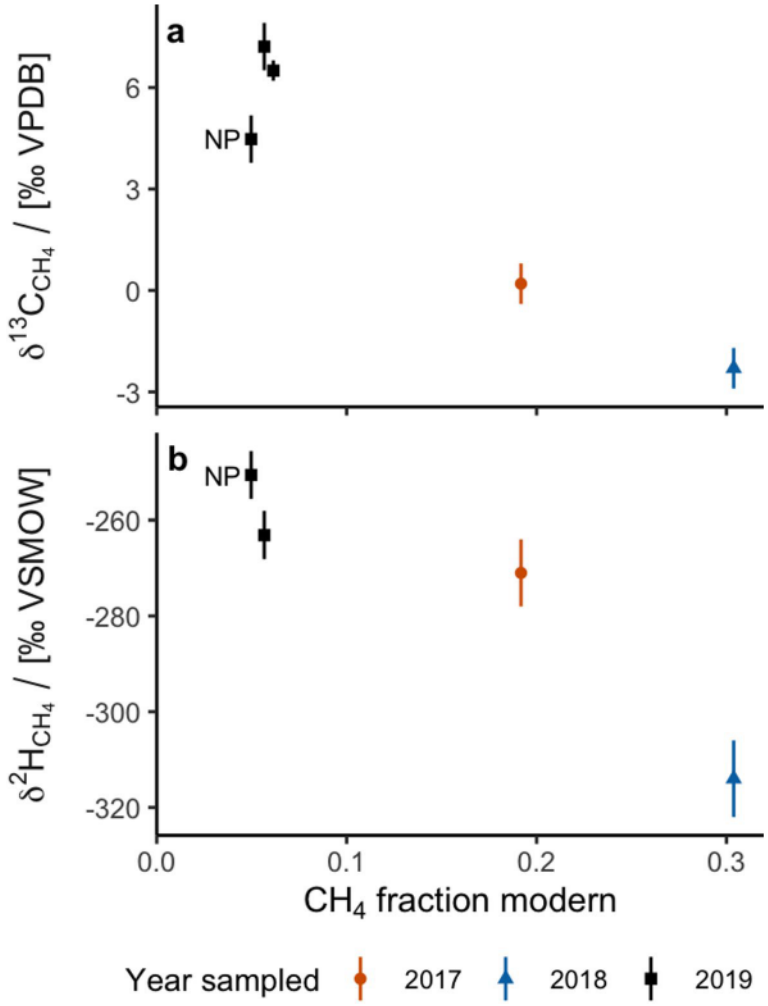


Fig. 1. Radiocarbon and stable isotopic composition of CH_4 at NSHQ14. "NP" indicates samples for which the well was not purged prior to sampling.

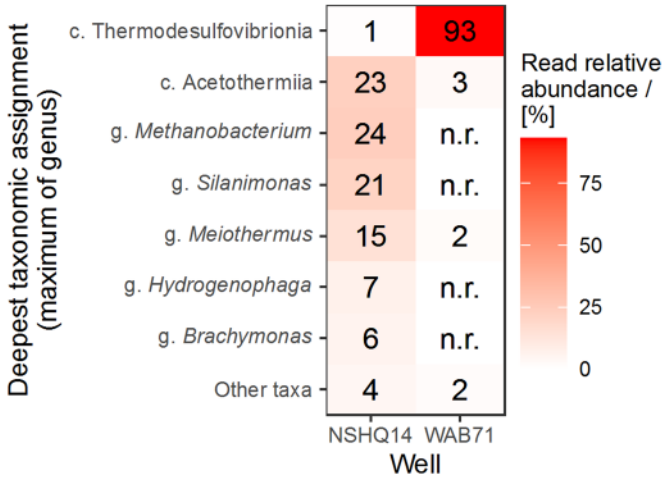


Fig. 2. 16S rRNA gene read relative abundances of 7 most abundant taxa inferred from DNA extracted from wells NSHQ14 (non-purged) and WAB71 sampled in 2019. Read relative abundances are reported as percentages rounded to the ones place. Cases when no reads of a taxon were detected in a sample are labeled "n.r."

Discussion

Carbon sources, rates, and mechanisms of CH_4 production

In the sample from well NSHQ14 in which the $F^{14}C_{CH_4}$ reached 0.304, 30 % or more of the CH_4 was recently (< 10 kyr BP) derived from atmospheric CO_2 (Table 4). This new CH_4 ^{14}C data set, which includes five gas samples from NSHQ14 obtained across three years of field work, sheds light on the drivers of isotopic variability within CH_4 previously identified in stable isotopic data from this site. Earlier studies proposed that positive, linear correlations between $\delta^{13}C_{CH_4}$ and $\delta^2H_{CH_4}$ in the Samail Ophiolite (Supplementary Fig. 4) may arise from microbial oxidation of CH_4 [29,33,51]. In contrast, we posit that the correlations of CH_4 $\delta^{13}C$, δ^2H, and $F^{14}C$ (Fig. 1) at NSHQ14 must result from mixing of at least two sources of CH_4 and do not require CH_4 oxidation. In the case of aerobic CH_4 oxidation, which is scarcely enzymatically reversible[52], oxidation would not be expected to affect the $F^{14}C$ of CH_4 ($F^{14}C$ is, by definition, corrected for mass-dependent fractionation [45]). Anaerobic CH_4 oxidation has greater reversibility and thus can cause isotopic equilibration between CH_4 and dissolved inorganic carbon ($\sum CO_2$)[53]. While this could conceivably introduce ^{14}C into CH_4, it is unlikely here because the stable isotopic composition of CH_4 at NSHQ14 is far from equilibrium with coexisting water, carbonate minerals, and itself (intramolecular equilibrium)[33]. Thus, we propose that the isotopic trends primarily stem from mixing of relatively ^{13}C- and ^2H-depleted, ^{14}C-rich ("young") CH_4 and relatively ^{13}C- and ^2H-enriched, ^{14}C-free CH_4. This is also consistent with microbiological data collected across multiple years of sampling that has not yielded evidence for abundant or active aerobic or anaerobic CH_4 oxidizing populations in NSHQ14[32,33,54–56]. However, we cannot entirely rule out some isotopic overprinting by CH_4 oxidation, which could have enriched the CH_4 samples in ^{13}C and ^2H without changing their $F^{14}C$.

Alongside isotopic compositions, molecular compositions provide insights into gas formation mechanisms. An abiotic component of CH_4 is strongly indicated by the presence of alkanes that have no known microbial production pathway (butane through hexane)[57] and the large ^{13}C enrichment observed in ethane and propane at NSHQ14 (Table 3; Supplementary Fig. 3)[33]. Debate on the nature of the abiotic source mechanism has centered around the relative contributions of CH_4 formed in fluid inclusions prior to the ophiolite's emplacement and CH_4 formed through ongoing, low-temperature processes[2,33]. Although NSHQ14 alkanes had relatively more CH_4 than the ideal ASF distribution (Supplementary Fig. 2), higher C_1 selectivity is a common occurrence in industrial Fischer–Tropsch (FT) reactions on Ru, Ni, and Co catalysts, which has been attributed to increased termination probability or methanation-specific reaction sites[58,59]. Thus, the molecular composition of NSHQ14 alkanes is consistent with Sabatier/FT-type reactions (with or without independent addition of microbial CH_4). The similarity in molecular composition of light hydrocarbons at NSHQ14 and Lost City (Supplementary Fig. 2), particularly from C_1 to C_3, suggests the potential for similar formation mechanisms across both sites. This is notable because fluid inclusions or higher temperature hydrothermal processes have been proposed as the dominant source mechanisms at Lost City[16,26,60]. However, the slopes of ASF fits between NSHQ14 and Lost City imply different apparent chain growth probabilities (α) of polymerization ($\alpha = 0.13$ for Lost City over C_2 to C_4 vs. 0.26 for NSHQ14 over C_2 to C_4 and 0.40 over C_2 to C_6). This could reflect different reaction temperatures or catalysts. Laboratory Sabatier/FT-type reaction experiments that used geological quantities of Ru have produced CH_4 and C_{2+} gases at temperatures as low as 25 °C, but the methods used for most of that study's C_{2+} measurements were semi-quantitative, which led those authors to refrain from attempting to fit their data to the ASF distribution[9]. Thus, further work is needed to determine molecular compositions of hydrocarbon gases that may be expected from low-temperature Sabatier/FT-type reactions with geological relevance to ophiolites.

Mass balance analysis can help to constrain uncertainties regarding the relative contributions of fluid inclusion decrepitation vs. low-temperature Sabatier/FT-type reactions to the abiotic CH_4 pool in ophiolites.

Such analysis was performed by Leong et al.[61], who also reported CH_4 and H_2 flux and gas compositional measurements from hyperalkaline springs in the Samail Ophiolite. The gas compositions, including noble gases, indicated that either decrepitation of fluid inclusions or low-temperature Sabatier/FT-type reactions associated with active serpentinization could have generated the H_2 and CH_4 outgassed from the springs they studied. In addition, Leong et al. calculated the rates and masses of peridotite alteration required to account for their gas flux data on the basis of thermodynamic reaction path modeling, catchment area and groundwater source depth estimates in Oman[62], and CH_4 concentrations in peridotite-hosted fluid inclusions from literature on other sites[16,63]. The serpentinization rates inferred from the gas flux data were within range of higher-temperature laboratory serpentinization experiments extrapolated to observed groundwater temperatures and rates inferred from crosscutting vein relationships and carbonate ^{14}C measurements from Oman boreholes[64]. From this, Leong et al. concluded that ongoing, low-temperature serpentinization can account for active out-gassing in hyperalkaline springs. Leong et al. did not preclude a fluid inclusion source component, although they did find that a mass of rock at least 20 times greater would be required to produce the same amount of CH_4 by fluid inclusion decrepitation. A similar conclusion was reached by Etiope and Oze[2]. In both studies, calculations were based on fluid inclusion-hosted CH_4 concentration data from locations outside the Samail Ophiolite. Future measurements of gas concentrations and isotopic compositions from fluid inclusions within Samail Ophiolite rocks would contribute meaningfully to the understanding of this area. Regardless, we are confident that any CH_4 potentially sourced from fluid inclusions is radiocarbon-dead[16]. Methane potentially formed through ongoing low-temperature hydrogenation of CO_2 derived from the mantle or decomposition of sedimentary rocks is also expected to be ^{14}C-free[20]. In these respects, the ^{14}C data reported by this study are inconclusive regarding the source of the proposed ^{14}C-free abiotic component of CH_4 within the study area. In any case, the question becomes whether the proposed ^{14}C-rich component of CH_4 found at NSHQ14 was formed through low-temperature abiotic or microbial processes.

Compositional and isotopic relationships between CH_4 and co-existing short-chain alkanes can be used to distinguish between abiotic and microbial CH_4 sources. Dominantly microbial gases tend to have relatively high $C_1/(C_2+C_3)$ because microbes that produce ethane or propane are rare[65,66], whereas ethane and propane are commonly produced through abiotic mechanisms[9,67–69]. In samples obtained from NSHQ14 in 2017 and 2018 (the samples with higher $F^{14}C_{CH_4}$), the $C_1/(C_2+C_3)$ was approximately twice that of samples from 2019 (Supplementary Fig. 5), indicating that the ^{14}C-rich CH_4 source component is associated with little to no ethane and propane relative to the ^{14}C-free component. This is consistent with a microbial source of ^{14}C-rich CH_4, although it does not preclude the presence of multiple abiotic CH_4 pools with distinct alkane distributions. Further, in contrast to the considerable isotopic variability observed in CH_4 at NSHQ14, the $\delta^{13}C$ values of ethane and propane were stable. In samples from 2019 and 2017 (the only samples for which $\delta^{13}C$ of ethane and propane were measured), the $\delta^{13}C$ values of ethane were within analytical uncertainty of each other, and $\delta^{13}C$ of propane varied by only 1.6 ‰ VPDB (Supplementary Fig. 3). In the same samples, $\delta^{13}C$ of CH_4 varied by 7 ‰ VPDB. This reinforces the idea that the ^{14}C-rich (and ^{13}C-depleted) CH_4 is produced independently from ethane and propane.

Microbiological data indicate the potential for microbial CH_4 production at NSHQ14. Sequences affiliated with *Methanobacterium*, a methanogen that can reduce CO_2 to CH_4 using H_2, formate or CO[46], were most abundant in 16S rRNA gene amplicons from 2019 NSHQ14 groundwater communities, accounting for 24% of reads (Fig. 2). In analogous samples obtained in other years, metagenomic and metatranscriptomic data have shown that genes involved in methanogenesis are not only present in the NSQH14 microbial community[32,54,56,70], but are also actively transcribed[55]. Further, microcosm assays on NSHQ14 groundwaters have shown rates of CH_4 production attributed to biology[32,54]. For example, microbial communities in groundwaters from NSHQ14 in 2017, for which we have paired natural abundance $F^{14}C_{CH_4}$ data, exhibited maximum potential rates of HCO_3^- reduction to CH_4 of 18 pmol mL^{-1} day^{-1} (equivalently, 6.6 µmol L^{-1} $year^{-1}$ [32]). Based on our independent measurement of $F^{14}C_{CH_4}$ of 0.192 in the same waters that year, which contained a total CH_4 concentration of 105 µmol L^{-1}, we calculate a concentration of modern CH_4 in that sample of 20.2 µmol L^{-1}. By dividing the concentration of modern CH_4 by the maximum rate of biological reduction of HCO_3^- to CH_4, we arrive at a potential time of 3.1 years for accumulation of the modern component of CH_4 from HCO_3^- through biological processes. Taken together, these data and calculations show that microbial processes have the potential to operate at sufficient rates to account for the modern component of CH_4 at NSHQ14.

Integrating chemistry and hydrology of fluids sampled from serpentinite-hosted wells

Having identified plausible sources for both the ^{14}C-rich and ^{14}C-free components of CH_4, we can examine why the relative proportions of CH_4 from these sources have differed across samples obtained in different years at NSHQ14. To do so, the hydrology of the well must be considered. A fundamental aspect of serpentinite aquifers is that groundwater dominantly flows through fissures and fractures with average spacing in the tens of meters, as opposed to micrometer-scale cracks and nanometer-scale pores within the serpentinite matrix[62,71]. From geophysical well logs obtained at ambient conditions in NSHQ14, Paukert[72] identified zones capable of hosting groundwater flow at depths of 70 m, 140 m, 180 m, and 250 m based on changes in temperature and, in some cases, caliper readings. Most of the 304 m-deep well had upward flow, while the lower 50 m had downward flow, suggesting a substantial inflow at 250 m depth. In a sampling campaign in 2020 (post-dating the sampling for this study), Fones et al.[54] installed an inflatable double packer system at NSHQ14 to attempt to pump deep groundwaters isolated from the surface. However, Fones et al. reported insufficient flow to pump water to the surface when the top packer was inflated at 30 m or 18 m depth. They did pump sufficient water when inflating the bottom packer at 30 m and leaving the upper packer uninflated, effectively pumping the interval 30 m to 9 m (the depth to water). Despite the shallow pumping interval, that water was still hyperalkaline (pH 11.3). Integrating the findings of Paukert[72] and Fones et al.[54] reveals that the channels (in the broad sense of the term)

feeding NSHQ14 can change between ambient and pumped conditions. These studies indicate that under pumped conditions, the well is fed primarily by regions of high hydraulic conductivity from 9 to 18 m depth, but under ambient conditions, the well is primarily fed from deeper regions.

The timing of pumping and the total volume of pumped water also can affect fluid chemistry substantially. Specifically, we found that waters sampled from NSHQ14 can become less representative of the end-member hyperalkaline composition of interest after prolonged pumping. For example, in 2019, immediately upon turning on the pump during our first sampling of NSHQ14, we recorded pH of 11.22, electrical conductivity of 2.88 mS cm^{-1}, temperature of 36.7 °C and *Eh* of −430. mV ($f_{O_2} = 8.16 \times 10^{-64}$bar). After purging the well, we found that the pH and electrical conductivity had decreased, and the *Eh* (and f_{O_2}) had increased (Table 1). We then began sampling fluids for chemical analysis. We likely pumped out much of the hyperalkaline water of interest and started drawing more water from more dilute, surficial sources as pumping progressed. Thus, we allowed NSHQ14 to recharge and repeated sampling 8 days later immediately upon resuming pumping. We refer to these samples as NSHQ14 "non-purged", or "NP". The non-purged sample returned to near the pH, electrical conductivity, and *Eh* values observed upon initial pumping of NSHQ14 8 days prior and before purging (Table 1). In addition, the non-purged sample had higher concentrations of major elements Na, Ca, and Cl. Further, the redox-active oxyanion SO_4^{2-} dropped in concentration from 47.3 μmol L^{-1} in the purged sample to 5.09 μmol L^{-1} in the non-purged sample (Table 1). Moreover, the concentrations of reduced gases H_2, CH_4, and short-chain alkanes were twice as high in the non-purged sample (Table 2), although the isotopic composition of CH_4 was overall similar between the purged and non-purged samples (Tablee 3, 4, and Fig. 1). Collectively, these findings suggest that the non-purged sample of NSHQ14 in 2019 is more representative of a reduced end-member hyperalkaline fluid type, while the purged sample had been mixed during pumping with a distinct fluid that is more oxidized and dilute. More broadly, we hypothesize that there are multiple aquifers accessed by NSHQ14 that contain isotopically distinct CH_4 pools. We propose that the isotopic variation in CH_4 from NSHQ14 across sampling events has been primarily caused by changes in the proportions of these CH_4 pools sampled due to differences in pumping technique.

Additional insights into fluid fluxes and fluid-rock-microbe interactions in the area surrounding NSHQ14 can be gleaned from petrologic investigations of cores from borehole BA3A, which was drilled 10 m away from NSHQ14 through the Oman Drilling Project[64]. BA3A was drilled to 300 m depth with 100% core recovery in January 2018, between the 2017 and 2018 sampling campaigns for this study. The six carbonate veins from cores from 5 to 9 m depth in BA3A that were analyzed for ^{14}C content had $F^{14}C$ of 0.004 to 0.078, corresponding to ^{14}C ages of 45 000 yr BP to 20 500 yr BP[64]. A detailed study of carbon geochemistry of several Oman Drilling Project boreholes including cores from BA3A found inorganic carbon contents of 500 ppm to 1000 ppm throughout most of BA3A[73]. While carbonate veins were most prevalent in the upper 100 m of BA3A, dispersed carbonates that were not microscopically identifiable, but were evidenced by the inorganic carbon content measurements, were present throughout the borehole. The three whole rock samples (ranging from 69.98 to 280.08 m depth) analyzed for ^{14}C content by Ternieten et al. had dispersed carbonate $F^{14}C$ values of 0.908 to 0.927, corresponding to ^{14}C ages of 771 yr BP to 608 yr BP. Co-existing non-carbonate (i.e., organic carbon, carbonaceous matter, or graphite) $F^{14}C$ values ranged from 0.273 to 0.366, corresponding to ^{14}C ages of 10 440 yr BP to 8083 yr BP.

Dating of groundwater recharge and dissolved constituents offers another lens through which to understand fluid fluxes and chemical turnover rates. Tritium measurements of NSHQ14 groundwaters have indicated pre-H-bomb recharge ages (before 1952)[74]. However, young ^{39}Ar apparent ages (90 yr to 720 yr) and dissolved inorganic carbon ^{14}C ages of 820 yr BP to 12 000 yr BP of hyperalkaline groundwater in the Samail Ophiolite underscore the rapid formation of the hyperalkaline water or its extensive mixing with more recently recharged waters[75]. In sum, from geochronological measurements on multiple substances, a picture is emerging of a more hydrologically active moderate (300 m) depth continental serpentinite aquifer system than was previously thought. Our CH_4 ^{14}C data indicate that this hydrologically active region also can host ongoing CH_4 production.

Ecological competitiveness of methanogens

In a study of hyperalkaline springs in the Samail Ophiolite, Howells et al.[76] identified a transition that occurred between SO_4^{2-} concentrations of 7.82 μmol L^{-1} and 10.67 μmol L^{-1}, above which hydrogenotrophic sulfate reduction had greater energy supplies than hydrogenotrophic methanogenesis, and below which hydrogenotrophic methanogenesis had greater energy supplies. Energy supply is a quantity describing the energy available to a chemotrophic metabolism in a mass of fluid, assuming a limiting reactant controls the total supply of energy that can be released from the reaction[76]. Consistent with calculated energy supplies, Howells et al. showed that sediment communities from hyperalkaline pools with SO_4^{2-} concentrations < 10 μmol L^{-1} were dominated by *Methanobacterium* whereas sediment communities from hyperalkaline pools with > 10 μmol L^{-1} SO_4^{2-} were dominated by Thermodesulfovibrionacea. Howells et al. proposed that sulfate-reducing bacteria may outcompete methanogens for H_2 in waters with > 10 μmol L^{-1} SO_4^{2-}, while methanogens predominate in waters with < 10 μmol L^{-1} SO_4^{2-} due to the greater energy supplies for methanogenesis in those waters.

While the Howells et al. model has apparent explanatory power, we consider its sole focus on dissolved inorganic carbon (and particularly the carbonate ion) as a carbon substrate to be an oversimplification. In the most hyperalkaline wells in the Samail Ophiolite, genomic and microcosm studies have shown that formate ($HCOO^-$) can be used as both an electron source and source of cytoplasmic CO_2 by "Type II" *Methanobacterium* through a metabolic pathway that presumably evolved to overcome the extreme inorganic carbon limitations within hyperalkaline serpentinite-hosted fluids[54,56]. Many sulfate reducing bacteria such as Thermodesulfovibrionia can also use formate for carbon assimilation and as an electron donor in sulfate reduction. Thus, future models building off the work of Howells et al. should add formate as a potential electron donor and as a potential electron acceptor. Nonetheless, if formate is an important substrate for methanogens and/or sulfate reducers, we would still expect there to be a threshold SO_4^{2-} concentration below which methanogens outcompete sulfate reducers.

Howells et al. identified this threshold in serpentinizing environments, even if the systematics underlying that threshold may differ from what they modeled.

Subsurface groundwaters accessed via wells WAB71 and NSHQ14 appear analogous to the hyperalkaline spring environments described by Howells et al. on either side of the 10 μmol L^{-1} SO_4^{2-} threshold. Groundwaters pumped from WAB71 in 2019 had a pH that was hyperalkaline (11.09; Table 1), but not quite as high as the highest pH waters sampled at NSHQ14 (11.2 to 11.4). In groundwaters pumped from WAB71 in 2019, the concentration of H_2 was below quantitation (< 3.29 μmol L^{-1}), and the concentration of CH_4 was 25.4 μmol L^{-1} (Table 2), both consistent with prior years of sampling[33,38]. The more than 2 orders of magnitude lower H_2 concentrations in groundwaters from WAB71 relative to NSHQ14 reflect starkly more reduced conditions at NSHQ14 ($f_{O_2} = 3.34 \times 10^{-59}$bar at WAB71 vs. 3.68×10^{-67}bar at NSHQ14 non-purged in 2019). Accordingly, SO_4^{2-} concentrations in WAB71 have been consistently in the range of 34 μmol L^{-1} to 60.8 μmol L^{-1} across five years of sampling since 2015 (Table 1)[33,38]; the lower (< 10 μmol L^{-1}) SO_4^{2-} concentrations that can be found at NSHQ14 depending on the pumping technique have never been observed at WAB71. Consistent with the repeated measurements of SO_4^{2-} at > 30 μmol L^{-1} in WAB71 groundwaters, DNA extracted from filter-concentrated biomass from groundwaters from WAB71 in 2019 had 16S rRNA gene reads dominated by the sulfate-reducing bacterial class Thermodesulfovibrionia (93% of reads), while the methanogen *Methanobacterium* was not detected (Fig. 2). Our finding of exclusively radiocarbon-dead CH_4 in WAB71 across two years of sampling (Table 4) may thus be a result of a paucity of active methanogens under conditions where microbial sulfate reducers benefit from greater energy supplies. In contrast, groundwaters with < 10 μmol L^{-1} SO_4^{2-} (and > 100 μmol L^{-1} H_2) do exist in some aquifers accessed by NSHQ14 (Tables 1 and 2), and it is in these aquifers where methanogenesis would be expected to outcompete sulfate reduction for the limited availability of electron acceptors. These geochemical conditions that energetically favor methanogenesis over sulfate reduction are exploited by methanogens, as evidenced by the elevated ^{14}C content of CH_4 at NSHQ14 (Table 4). The fluids sampled from other wells in this study, NSHQ04 and CM2A, had $F^{14}C_{CH_4} < 0.01$ (Table 4), > 100 μmol L^{-1} SO_4^{2-} and orders of magnitude lower H_2 concentrations than NSHQ14, which is consistent with this hypothesis. Broader geochemical context on these wells is reviewed in Supplementary Discussion 1.

Multiple systems of CH_4 generation in low-temperature serpentinizing settings

By comparing studies of serpentinitization-influenced groundwaters accessed via wells to those on vent fluids, a broader perspective comes into view of multiple systems of CH_4 generation. Among studies of ^{14}C CH_4 in serpentinites, the study of wells in Hakuba Happo, Japan by Suda et al.[21] had the most similar sampling methods to the present study. The findings of Suda et al. differ from ours in that they observed a maximum CH_4 $F^{14}C$ of 0.0065 ± 0.0002. In comparison, carbonate minerals that had accumulated on the water pumping pipe in one of the Happo wells had a mean $F^{14}C$ of 0.5622. Using the carbonates on the pipe as a proxy for the ^{14}C content of inorganic carbon in the aquifer, Suda et al. calculated that the contribution of CH_4 formed from inorganic carbon in the groundwater was less than 1.2% of the total CH_4 pool. Rather, Suda et al. concluded that most of the CH_4 in the sampled groundwaters was formed at > 200 °C and migrated from depth through faults into the groundwaters or was entrained from fluid inclusions. The other previously published ^{14}C measurements on CH_4 sampled from ophiolites were sampled from dry gas vents (Philippines[17] and Turkey[18]) or from gas bubbles flowing as a separate phase within surface spring waters (Spain[19] and Italy[20]). Both dry gas vents and bubbling waters were sampled in the Bulqizë chromite mine in Albania[22]. The bubbling gas manifestations have been interpreted as being formed at depth through gas-phase reactions and then migrating along faults into the spring waters; in other words, the gas generation processes were considered independent of those controlling water chemistry[20]. In this regard, previous ophiolite vent CH_4 ^{14}C data are fundamentally different from those we report here because our samples represent CH_4 dissolved in groundwater and because, in the case of well NSHQ14, we find strong isotopic, aqueous geochemical, and microbiological evidence for a substantial (minimum 5%; Fig. 1) portion of CH_4 formation *within* the groundwater. Methane formation pathways inside and outside aquifer fluids as sampled via wells are illustrated in Fig. 3.

The Samail Ophiolite is unique in having many wells exceeding 300 m depth that have been drilled by the Omani government as part of groundwater resource surveys and the recent Oman Drilling Project scientific drilling program[64]. This study is part of a body of work seeking to characterize the hydrology, chemistry, and biology of subsurface fluids accessed through those wells. Well studies and natural seep studies are complementary and have tradeoffs such as the ability to generate hydrologic and petrologic data versus the degree of perturbation of the natural system involved. Methane ^{14}C analyses on Samail Ophiolite seep samples were beyond the scope of our study but would be interesting to pursue in future studies to advance understanding of the fluid dynamics, chemistry, and microbiology of serpentinites. For example, to test hypotheses about the effect of groundwater redox state (as reflected in H_2 and SO_4^{2-} concentrations) on the activities of microbial sulfate reducers and methanogens[76], springs across a range of redox states could be targeted for CH_4 sampling and ^{14}C analysis. The natural springs for which CH_4 was ^{14}C-free (in Spain[19] and Italy[20,78]) contained water with < 10 μmol L^{-1} H_2 concentrations. This could either be due to low-H_2 (mildly reduced) waters along the flow path of the springs' source waters, or because of microbial H_2 oxidation during fluid ascent. If the former, those spring waters would not have experienced the extremely reduced (> 100 μmol L^{-1} H_2) conditions present at NSHQ14, which may be a key driver of methanogenic activity. Spring waters spanning a wide range of redox conditions do exist in the Samail Ophiolite (e.g., Shumayt and Dima[35,76]), which could offer a natural testbed for these hypotheses.

While most of our discussion has focused on ophiolites, CH_4-rich vents influenced by low-temperature serpentinization at the Lost City Hydrothermal Field at the Mid-Atlantic Ridge presents an opportunity for broader comparative analysis of CH_4 ^{14}C dynamics. Lost City vent fluids have an order of magnitude higher concentrations of CH_4 and H_2 than in NSHQ14 groundwaters and have similarly low endmember $\sum CO_2$ concentrations of < 10 μmol kg^{-1} [4,26,33,72,79,80]. Based on a flow path within the temperature limits of life in the

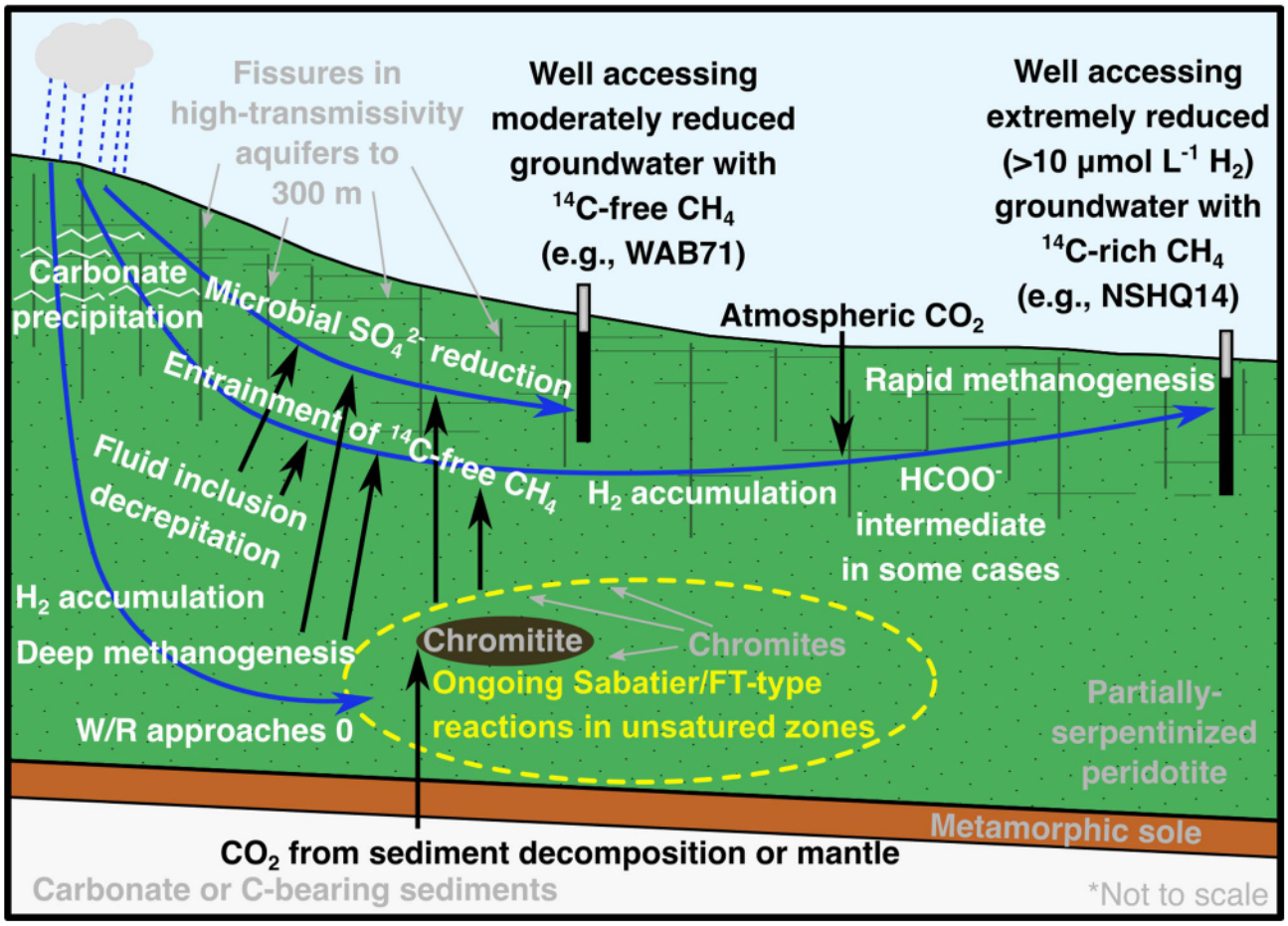


Fig. 3. Cross-sectional representation of fluid flow pathways and multiple systems of CH_4 generation within ophiolites, incorporating concepts from[9,20,28,33,38,77]. *Abbreviations:* "FT" = "Fischer – Tropsch"; "W/R" = "water / rock ratio".

carbonate chimneys and shallow basement rocks of a few tens of meters and making informed assumptions about volumetric microbial cell densities and cell specific CH_4 production rates, Bradley and Summons [81] estimated an upper limit on microbial CH_4 concentration of ~ 10–30 µmol L^{-1} in Lost City vent fluids. A similar estimate can be obtained from ^{14}C data. The CH_4 samples reported by Proskurowski et al.[26] had high-end $F^{14}C$ values of ~ 0.005, and assuming microbial CH_4 has a similar upper-bound $F^{14}C$ as lipids attributed to methanogens (pentamethylicosanes) in vent chimneys of 0.5[82], an upper limit of ~ 1% microbial CH_4 in the total CH_4 pool is obtained. Based on total CH_4 concentrations of ~ 1 mmol L^{-1}, it follows that the concentration of microbial CH_4 at Lost City may reach ~ 10 µmol L^{-1}, which is in the range estimated by Bradley and Summons[81]. This is in the same order of magnitude as the concentration of modern, presumably microbial CH_4 we report in samples from well NSHQ14 (e.g., 20.2 µmol L^{-1} in 2017). Thus, the concentrations of microbial CH_4 at Lost City and NSHQ14 may be similar, but the higher concentration of abiotic CH_4 at Lost City obscures the microbial CH_4 signal there.

The comparison with Lost City highlights the depth of microbial habitability and availability of carbon as important factors limiting microbial (methanogenic) activity in subseafloor hydrothermal serpentinizing systems. This raises the question of whether similar or different factors control methanogenic activity in ophiolites. The geothermal gradient derived from NSHQ14 well logs is 25.1 °C km^{-1} [83]. The highest temperature at which cell proliferation has been recorded is 122 °C, and these cells were methanogens[84]. Based on these values, we calculate a potential depth of methanogenic life in Samail Ophiolite of 3.5 km. This implies a large zone of potential methanogenic activity (> 10X deeper than NSHQ14) and suggests that temperature is not the most important control on methanogenic activity in the Samail Ophiolite. A more important limit on methanogenic activity in the Samail Ophiolite (that also is important at Lost City) is the availability of C. Our study shows that where H_2-rich waters contact atmospheric CO_2, methanogens are poised to rapidly generate methane. However, our study does not rule out the possibility of deep (1 km or more) methanogenesis as a source of ^{14}C-free CH_4 formed from non-atmospheric C sources or formed and transported to springs or wells over > 50 000 yr timescales.

Another potential limit on methanogenic activity (and life in general) is the presence of water. Inherent to serpentinization is net consumption of water to mineral hydration and conversion to H_2, which implies that at sufficiently low water/rock ratios, the system eventually can "dry out" into gas phase H_2 (while the vast majority

of CO_2 in the initial fluid would have been lost to carbonates). If CO_2 enters such water-unsaturated zones from other rock formations, Sabatier/FT-type reactions could occur there while microbial methanogenesis is suppressed (Fig. 3)[20]. However, the spatial extent of water-unsaturated zones in ophiolites is unknown and should be further studied, for example, by drilling deep boreholes targeting hypothesized pressurized gas accumulations.

Conclusion

This study documents CH_4 exsolved from groundwaters accessed via four serpentinite-hosted wells in the Samail Ophiolite having ^{14}C contents ranging from radiocarbon dead to 0.304 fraction modern. This finding implies that, in the sample with the highest fraction modern (from well NSHQ14), $> 30\%$ of that CH_4 was produced from atmospheric CO_2 within the last 10 000 years. By re-sampling the groundwaters during annual field campaigns spanning three years, we assessed temporal variability in the ^{14}C content of CH_4. In doing so, we observed negative correlations between $F^{14}C$ and the ratios of heavy to light stable isotopes within CH_4 (reported as $\delta^{13}C$ and $\delta^{2}H$) from well NSHQ14. This trend suggests that the CH_4 sampled at this well contained mixtures of at least two CH_4 source components including an ancient, isotopically "heavy" CH_4 component and a young, isotopically "light" CH_4 component. An abiotic component of relatively ^{13}C-enriched CH_4 at NSHQ14 is strongly indicated by the co-existence of ^{13}C-enriched ethane and propane, whose $\delta^{13}C$ values were practically invariant across sampling events. Integrating geochemical, isotopic, and numerous microbiological lines of evidence, we conclude that microbial methanogenesis is the most likely source of the ^{14}C-rich component of CH_4 at NSQH14. This adds quantitative strength to prior studies indicating that methanogens can indeed be active even at $pH > 11$ and with extremely low $\sum CO_2$. In a separate well in the ophiolite, WAB71, the presence of radiocarbon-dead CH_4, higher SO_4^{2-} concentrations, lower H_2 concentrations, and higher abundances of sulfate reducing bacteria relative to methanogenic archaea suggest that microbial sulfate reduction is dominant in groundwaters surrounding that well, outcompeting methanogenesis. Consistent with prior bioenergetic models, we find extremely reduced conditions as reflected in H_2 and SO_4^{2-} concentrations may be required for the accumulation of microbial CH_4 in ophiolites. Our findings differ from but complement previous natural seep studies that found mostly radiocarbon-dead CH_4 in ophiolites because the natural seeps were interpreted to source gas-phase CH_4 from regions of the ophiolite subsurface devoid of liquid water. Considered alongside other geochronometers, CH_4 ^{14}C reveals a striking degree of hydrologic and microbial activity of serpentinite aquifers to depths of 300 m. Geothermal gradients suggest methanogens could be poised to generate CH_4 as deep as 3.5 km in the Samail Ophiolite, with rates likely limited by the availability of carbon and water. Our finding of rapid microbial CH_4 formation contributes to the understanding of the baseline state of the natural serpentinite systems, which should be considered in engineering approaches to produce H_2 and/or store CO_2 in such systems[3,85].

Methods

Pumping and in-field measurements

The groundwaters analyzed in this study were sampled from four wells during field campaigns in February 2017, February 2018, and January 2019. Information on well location and construction are given in Nothaft et al.[33]. Fluids were sampled with a submersible pump (Grundfos SQ 2–85). The pumping depths are reported in Table 1 and Table 4. Each well was pumped for $\geq$ 20 min prior to sampling. Sampling commenced once fluid pH and conductivity measurements stabilized. The only exception to this was a replicate from NSHQ14 that was not purged prior to sampling, which is labeled as "NP", or indicated in table footnotes, where applicable. This was done as a test of the effect of purging methods on water chemical composition. The NP sampling was conducted 8 days after a normal sampling of NSHQ14, when the well was pumped for 233 min at a rate of 20 L min^{-1} prior to sample acquisition.

^{14}C analysis of CH_4

CH_4 was prepared for ^{14}C analysis at the Institute for Alpine and Arctic Research (INSTAAR) Laboratory for AMS Radiocarbon Preparation and Research at CU-Boulder. The INSTAAR CH_4 preparation line is based on the designs of Lowe et al.[86] and Petrenko et al.[87]. Gas was extracted from 37 mL blue butyl-stoppered serum vials by flowing C-free air at 100 mL min^{-1} through the vial and onto the main preparation line for 15 min, using BD PrecisionGlide™ needles (0.124 cm outer diameter, 3.8 cm length) to puncture the stopper. Extracted gas flowed across a series of cryogenic traps to remove water and CO_2. CO was quantitatively oxidized over Sofnocat® catalyst, and the resultant CO_2 was removed by additional cryogenic trapping. Residual sample was then combusted over platinized glass wool to yield CO_2 from (primarily) CH_4. The yield was quantified and the process CO_2 transferred to flame-sealed tubes for eventual graphitization and measurement by accelerator mass spectrometry at the University of California—Irvine using the procedures of Turnbull et al.[43].

"CH_4" prepared for ^{14}C analysis at INSTAAR technically reflects all combustible gases after removal of CO and CO_2, which includes $C_2 - C_6$ alkanes. Isolation of CH_4 through gas chromatography (GC) is not employed on the CH_4 radiocarbon prep line at INSTAAR because it was designed for atmospheric samples in which CH_4 is the dominant hydrocarbon. Similarly, we calculated that the potential uncertainty in $^{14}C/^{12}C$ introduced by non-methane hydrocarbons is negligible in our samples because CH_4 contained > 99 mol % of C within the total gaseous hydrocarbon pool in the samples (Supplementary Note 1).

To independently verify our methods, a replicate gas sample from one of the studied wells (NSHQ14) was sent to Isotech laboratories, where CH_4 was quantitatively separated from the other components by gas chromatography and then converted to CO_2, which was purified and captured in a Pyrex tube. This captured

CO_2 was sent to National Ocean Sciences Accelerator Mass Spectrometry (NOSAMS), where it was converted to graphite, which was then analyzed for its $^{14}C/^{12}C$ ratio.

Chemical and stable isotopic analyses of fluids

To analyze aqueous concentrations of non-carbonaceous chemical species, samples were collected by passing groundwater through a $0.2\,\mu m$ filter into polypropylene conical tubes. Aqueous concentrations were measured by inductively coupled plasma atomic emission spectroscopy (repeatability as median relative standard deviation of 3 % for most ions). Aqueous concentrations of F^- Cl^-, SO_4^{2-}, Br^-, and NO_3^- were measured by ion chromatography (analytical uncertainty of 5 %). The concentration and $\delta^{13}C$ of dissolved inorganic C ($\sum CO_2$) were measured by acidification of water samples and transfer of resultant CO_2 (g) via a Thermo Fisher GasBench II to a Thermo Delta V Plus isotope ratio mass spectrometer[88].

Groundwaters and gases dissolved therein were sampled via syringe from a luer-lok port on the pump manifold. 60. mL of this water was then passed through a $0.2\,\mu m$ filter and needle into an evacuated 117 mL glass vial capped with a blue chlorobutyl rubber stopper and crimp top. These are referred to as "headspace" samples. In addition, gases were sampled with the bubble strip method[89]. H_2, CH_4, and CO concentrations in this study are reported from headspace samples due to the better accuracy of this method versus the bubble strip method, as determined in comparisons by the authors. Ethane through hexane concentrations were determined from the bubble strip samples because of the lower detection limit offered by bubble strip samples and were normalized to the headspace gas samples through the CH_4 concentration and assumption of constant C_1/C_n ratio of both sample types, where C_n is an alkane of n C atoms. Gas concentrations were determined according to the methods of Nothaft et al.[33].

Bulk stable isotope analyses of CH_4 and co-occurring alkane gases were conducted at the University of Colorado—Boulder by GC/C/Pyr/IRMS using a Trace 1310 GC equipped with an Agilent J & W GS-CarbonPLOT column (30 m length, 0.32 mm ID, $3.0\,\mu m$ film) coupled to a Thermo Scientific MAT253 IRMS. Three CH_4 isotope standards purchased from Airgas (uncertainties of ± 0.3 ‰ for $\delta^{13}C$ and ± 5 ‰ for δ^2H) and three additional standards obtained from the U.S. Geological Survey (uncertainties of ± 0.2 ‰ for $\delta^{13}C$ and ± 3 ‰ for δ^2H) were used for calibration. Over the range of peak amplitudes of analyses reported here, the repeatability expressed as $1\,s$ on analyses of standards is ± 0.2 ‰ for $\delta^{13}C$ and ± 3 ‰ for δ^2H. The analytical uncertainty (accuracy) expressed as 1 standard error on a 3-point calibration was 0.4 ‰ to 0.7 ‰ or $\delta^{13}C$ and 4 ‰ to 5 ‰ for δ^2H (Supplementary Note 1). As a consistency check, an additional analysis of $\delta^{13}C_{CH_4}$ of one sample was performed by GC/C/IRMS by Isotech laboratories with a precision of 0.3 ‰ ($1\,\sigma$).

16S rRNA gene sequencing and analysis

Biomass for DNA extraction was concentrated by pumping 5 L to 20 L of groundwater through Millipore polycarbonate inline filters ($0.22\,\mu m$ pore diameter, 47 mm filter diameter). Filters were placed in cryovials, transported frozen in liquid N_2, and stored in a $-70\,^\circ C$ freezer until extraction. DNA was extracted from one quarter subsamples of each filter using a Qiagen PowerSoil DNA extraction kit. The V4 hypervariable region of the 16S SSU rRNA gene was amplified from purified DNA by PCR. PCR was performed in triplicate reactions using the 515F/806R primer pair at an annealing temperature of 50 °C, as described previously[90]. Amplicons from triplicate reactions were pooled, and adapters were added in triplicate reactions via five cycles of nested PCR (following the same conditions as above) with 515F/816R primers modified to include Illumina adapters. Amplicons from triplicate reactions were pooled and purified using the Wizard® PCR Preps DNA Purification System (Promega Corp.). Sequencing on the 2×150 Illumina Miseq platform was performed at the UW-Madison Biotechnology Center DNA Sequencing Facility.

Demultiplexed fastq files were quality filtered using Figaro v1.1.1[91] and the DADA2 v1.16 R package[92]. Amplicon sequence variants were assigned taxonomy to the genus level using the RDP classifier[93] trained on the Silva SSU 138 reference database[94] using the DADA2 assignTaxonomy function. Sequences assigned to mitochondria, chloroplast, and Eukaryota, or not assigned at the domain level (collectively < 1 % of sequences), were removed. DNA sequence data processing codes are archived on Zenodo 95.

Data availability

Data (in Excel format) presented in this paper (as well as additional data on analytical uncertainties and trace element concentrations) are archived on Zenodo (https://doi.org/10.5281/zenodo.17593505). DNA sequence data are accessible on the NCBI Short Read Archive under accession PRJNA1261609.

Received: 11 July 2025; Accepted: 24 December 2025
Published online: 19 January 2026

References

1. Kelemen, P. B. et al. Rates and Mechanisms of Mineral Carbonation in Peridotite: Natural Processes and Recipes for Enhanced, in situ CO2 Capture and Storage. *Annu. Rev. Earth Planet. Sci.* **39**(39), 545–576 (2011).
2. Etiope, G. & Oze, C. Microbial vs abiotic origin of methane in continental serpentinized ultramafic rocks: A critical review and the need of a holistic approach. *Appl. Geochem.* **143**, 105373 (2022).
3. Templeton, A. S. et al. Low-temperature hydrogen production and consumption in partially-hydrated peridotites in Oman: implications for stimulated geological hydrogen production. *Front. Geochem.* **2**, 1366268 (2024).
4. Leong, J. A. M. & Shock, E. L. Thermodynamic constraints on the geochemistry of low-temperature, continental, serpentinization-generated fluids. *Am. J. Sci.* **320**, 185–235 (2020).
5. Shock, E. L. Chapter 5 Chemical environments of submarine hydrothermal systems. *Orig. Life Evol. Biosph.* **22**, 67–107 (1992).
6. McCollom, T. M. Abiotic methane formation during experimental serpentinization of olivine. *Proc. Natl. Acad. Sci.* 201611843 (2016) https://doi.org/10.1073/pnas.1611843113.

7. Medina, J. C., Butala, S. J., Bartholomew, C. H. & Lee, M. L. Low temperature iron- and nickel-catalyzed reactions leading to coalbed gas formation. *Geochim. Cosmochim. Acta* **64**, 643–649 (2000).
8. Taran, Y. A., Kliger, G. A., Cienfuegos, E. & Shuykin, A. N. Carbon and hydrogen isotopic compositions of products of open-system catalytic hydrogenation of CO2: Implications for abiogenic hydrocarbons in Earth's crust. *Geochim. Cosmochim. Acta* **74**, 6112–6125 (2010).
9. Etiope, G. & Ionescu, A. Low-temperature catalytic CO 2 hydrogenation with geological quantities of ruthenium: a possible abiotic CH 4 source in chromitite-rich serpentinized rocks. *Geofluids* **15**, 438–452 (2015).
10. Barbier, S. *et al.* A Review of H2, CH4, and Hydrocarbon Formation in Experimental Serpentinization Using Network Analysis. *Front. Earth Sci.* **8**, (2020).
11. Ruiz, P. et al. Abiotic Transformation of H2 and CO2 into Methane on a Natural Chromitite Rock. *ACS Earth Space Chem.* **5**, 1695–1708 (2021).
12. Pappalardo, L., Buono, G., Procesi, M. & Etiope, G. The link between ophiolitic chromitites, natural hydrogen and methane: Insights from 3D microtomography. *Chem. Geol.* **676**, 122575 (2025).
13. Kelley, D. S. Methane-rich fluids in the oceanic crust. *J. Geophys. Res. Solid Earth* **101**, 2943–2962 (1996).
14. Kelley, D. S. & Früh-Green, G. L. Abiogenic methane in deep-seated mid-ocean ridge environments: Insights from stable isotope analyses. *J. Geophys. Res. Solid Earth* **104**, 10439–10460 (1999).
15. Wang, D. T., Reeves, E. P., McDermott, J. M., Seewald, J. S. & Ono, S. Clumped isotopologue constraints on the origin of methane at seafloor hot springs. *Geochim. Cosmochim. Acta* **223**, 141–158 (2018).
16. Klein, F., Grozeva, N. G. & Seewald, J. S. Abiotic methane synthesis and serpentinization in olivine-hosted fluid inclusions. *Proc. Natl. Acad. Sci.* **116**, 17666–17672 (2019).
17. Abrajano, T. A. et al. Geochemistry of reduced gas related to serpentinization of the Zambales ophiolite. *Philippines. Appl. Geochem.* **5**, 625–630 (1990).
18. Etiope, G. & Schoell, M. Abiotic Gas: Atypical. *But Not Rare. Elements* **10**, 291–296 (2014).
19. Etiope, G. et al. Abiotic methane seepage in the Ronda peridotite massif, southern Spain. *Appl. Geochem.* **66**, 101–113 (2016).
20. Etiope, G. & Whiticar, M. J. Abiotic methane in continental ultramafic rock systems: Towards a genetic model. *Appl. Geochem.* **102**, 139–152 (2019).
21. Suda, K. et al. The origin of methane in serpentinite-hosted hyperalkaline hot spring at Hakuba Happo, Japan: Radiocarbon, methane isotopologue and noble gas isotope approaches. *Earth Planet. Sci. Lett.* **585**, 117510 (2022).
22. Truche, L. et al. A dynamic H2 system with multi-source methane in chromitite-rich ophiolitic settings. *Geochim. Cosmochim. Acta* **409**, 281–307 (2025).
23. Price, R. E. et al. Methane cycling in the Prony Bay Hydrothermal Field, New Caledonia: insights from clumped CH4 isotopologues and 14C-CH4. *Astrobiol. Sci. Conf. (AbSciCon)* **2024**, 304–402 (2024).
24. Kelley, D. S. et al. An off-axis hydrothermal vent field near the Mid-Atlantic Ridge at 30° N. *Nature* **412**, 145–149 (2001).
25. Seyfried, W. E., Pester, N. J., Tutolo, B. M. & Ding, K. The Lost City hydrothermal system: Constraints imposed by vent fluid chemistry and reaction path models on subseafloor heat and mass transfer processes. *Geochim. Cosmochim. Acta* **163**, 59–79 (2015).
26. Proskurowski, G. et al. Abiogenic Hydrocarbon Production at Lost City Hydrothermal Field. *Science* **319**, 604–607 (2008).
27. Kelemen, P. B. & Matter, J. In situ carbonation of peridotite for CO2 storage. *Proc. Natl. Acad. Sci.* **105**, 17295–17300 (2008).
28. Neal, C. & Stanger, G. Past And Present Serpentinisation of Ultramafic Rocks; An Example from the Semail Ophiolite Nappe of Northern Oman. in *The Chemistry of Weathering* 249–275 (The Open University, Dordrecht, 1985). https://doi.org/10.1007/978-94-009-5333-8_15.
29. Miller, H. M. et al. Modern water/rock reactions in Oman hyperalkaline peridotite aquifers and implications for microbial habitability. *Geochim. Cosmochim. Acta* **179**, 217–241 (2016).
30. Fritz, P., Clark, I. D., Fontes, J.-C., Whiticar, M. J. & Faber, E. Deuterium and 13C evidence for low temperature production of hydrogen and methane in a highly alkaline groundwater environment in Oman. in Water-rock interaction : proceedings of the 7th International Symposium on Water-Rock Interaction : WRI-7, Park City, Utah, USA, 13–18 July 1992 (eds Kharaka, Y. K. & Maest, A. S.) 793–796 (Balkema, Rotterdam, 1992).
31. Etiope, G., Judas, J. & Whiticar, M. J. Occurrence of abiotic methane in the eastern United Arab Emirates ophiolite aquifer. *Arab. J. Geosci.* **8**, 11345–11348 (2015).
32. Fones, E. M. *et al.* Physiological adaptations to serpentinization in the Samail Ophiolite, Oman. *ISME J.* (2019) https://doi.org/10.1038/s41396-019-0391-2.
33. Nothaft, D. B. et al. Geochemical, Biological, and Clumped Isotopologue Evidence for Substantial Microbial Methane Production Under Carbon Limitation in Serpentinites of the Samail Ophiolite. *Oman. J. Geophys. Res. Biogeosci.* **126**, 1–30 (2021).
34. Templeton, A. S. et al. Accessing the Subsurface Biosphere Within Rocks Undergoing Active Low-Temperature Serpentinization in the Samail Ophiolite (Oman Drilling Project). *J. Geophys. Res. Biogeosci.* **126**, 1–30 (2021).
35. Leong, J. A. *et al.* H2 and CH4 outgassing rates in the Samail ophiolite, Oman: Implications for low-temperature, continental serpentinization rates. *Geochim. Cosmochim. Acta* (2023) https://doi.org/10.1016/j.gca.2023.02.008.
36. Vacquand, C. et al. Reduced gas seepages in ophiolitic complexes: Evidences for multiple origins of the H2-CH4-N2 gas mixtures. *Geochim. Cosmochim. Acta* **223**, 437–461 (2018).
37. Leong, J. A. M. *et al.* Theoretical Predictions Versus Environmental Observations on Serpentinization Fluids: Lessons From the Samail Ophiolite in Oman. *J. Geophys. Res. Solid Earth* **126**, (2021).
38. Rempfert, K. R. *et al.* Geological and Geochemical Controls on Subsurface Microbial Life in the Samail Ophiolite, Oman. *Front. Microbiol.* **8**, (2017).
39. Flory, P. Molecular Size Distribution in Linear Condensation Polymers1. *J. Am. Chem. Soc.* **58**, 1877–1885 (1936).
40. Anderson, R. B. Ch. 5 Mechanism of the Fischer-Tropsch Synthesis. in *The Fischer-Tropsch Synthesis* (Academic Press, Inc., Orlando, FL USA, 1984).
41. Etiope, G. & Sherwood Lollar, B. Abiotic methane on earth. *Rev. Geophys.* **51**, 276–299 (2013).
42. Milkov, A. V. & Etiope, G. Revised genetic diagrams for natural gases based on a global dataset of >20,000 samples. *Org. Geochem.* **125**, 109–120 (2018).
43. Turnbull, J. C. *et al.* A new high precision 14CO2 time series for North American continental air. *J. Geophys. Res. Atmospheres* **112**, (2007).
44. Stuiver, M. & Polach, H. A. Discussion Reporting of ^{14}C Data. *Radiocarbon* **19**, 355–363 (1977).
45. Reimer, P. J., Brown, T. A. & Reimer, R. W. Discussion: Reporting and Calibration of Post-Bomb 14 C Data. *Radiocarbon* **46**, 1299–1304 (2004).
46. Boone, D. R. Methanobacterium. in *Bergey's Manual of Systematics of Archaea and Bacteria* 1–8 (John Wiley & Sons, Ltd, 2015). https://doi.org/10.1002/9781118960608.gbm00495.
47. Sekiguchi, Y. *et al.* Thermodesulfovibrio aggregans sp. nov. and Thermodesulfovibrio thiophilus sp. nov., anaerobic, thermophilic, sulfate-reducing bacteria isolated from thermophilic methanogenic sludge, and emended description of the genus Thermodesulfovibrio. *Int. J. Syst. Evol. Microbiol.* **58**, 2541–2548 (2008).
48. Maki, J. S. Thermodesulfovibrio. in *Bergey's Manual of Systematics of Archaea and Bacteria* 1–9 (John Wiley & Sons, Ltd, 2015). https://doi.org/10.1002/9781118960608.gbm00781.
49. Nothaft, D. B. danote/Oman-14CH4: Oman-14CH4 zenodo. Zenodo https://doi.org/10.5281/zenodo.17593505 (2025).

50. Hanson, R. S. & Hanson, T. E. Methanotrophic bacteria. *Microbiol. Rev.* **60**, 439–471 (1996).
51. Miller, H. M. et al. Large carbon isotope variability during methanogenesis under alkaline conditions. *Geochim. Cosmochim. Acta* **237**, 18–31 (2018).
52. Wang, D. T., Welander, P. V. & Ono, S. Fractionation of the methane isotopologues 13CH4, 12CH3D, and 13CH3D during aerobic oxidation of methane by Methylococcus capsulatus (Bath). *Geochim. Cosmochim. Acta* **192**, 186–202 (2016).
53. Yoshinaga, M. Y. et al. Carbon isotope equilibration during sulphate-limited anaerobic oxidation of methane. *Nat. Geosci.* **7**, 190–194 (2014).
54. Fones, E. M. et al. Diversification of methanogens into hyperalkaline serpentinizing environments through adaptations to minimize oxidant limitation. *ISME J.* **15**, 1121–1135 (2021).
55. Kraus, E. A. et al. Molecular Evidence for an Active Microbial Methane Cycle in Subsurface Serpentinite-Hosted Groundwaters in the Samail Ophiolite. *Oman. Appl. Environ. Microbiol.* **87**, e02068-e2120 (2021).
56. Colman, D. R., Templeton, A. S., Spear, J. R. & Boyd, E. S. Microbial ecology of serpentinite-hosted ecosystems. *ISME J.* **19**, wraf029 (2025).
57. Formolo, M. The Microbial Production of Methane and Other Volatile Hydrocarbons. in *Handbook of Hydrocarbon and Lipid Microbiology* 113–126 (Springer Berlin Heidelberg, 2010). https://doi.org/10.1007/978-3-540-77587-4.
58. Puskas, I. & Hurlbut, R. S. Comments about the causes of deviations from the Anderson–Schulz–Flory distribution of the Fischer-Tropsch reaction products. *Catal. Today* **84**, 99–109 (2003).
59. Förtsch, D., Pabst, K. & Groß-Hardt, E. The product distribution in Fischer-Tropsch synthesis: An extension of the ASF model to describe common deviations. *Chem. Eng. Sci.* **138**, 333–346 (2015).
60. Labidi, J. et al. Methane thermometry in deep-sea hydrothermal systems: Evidence for re-ordering of doubly-substituted isotopologues during fluid cooling. *Geochim. Cosmochim. Acta* **288**, 248–261 (2020).
61. Leong, J. A. et al. H2 and CH4 outgassing rates in the Samail ophiolite, Oman: Implications for low-temperature, continental serpentinization rates. *Geochim. Cosmochim. Acta* **347**, 1–15 (2023).
62. Dewandel, B. et al. A conceptual hydrogeological model of ophiolite hard-rock aquifers in Oman based on a multiscale and a multidisciplinary approach. *Hydrogeol. J.* **13**, 708–726 (2005).
63. Grozeva, N. G., Klein, F., Seewald, J. S. & Sylva, S. P. Chemical and isotopic analyses of hydrocarbon-bearing fluid inclusions in olivine-rich rocks. *Philos. Trans. R. Soc. Math. Phys. Eng. Sci.* **378**, 20180431 (2020).
64. Kelemen, P. B. et al. Initial Results From the Oman Drilling Project Multi-Borehole Observatory: Petrogenesis and Ongoing Alteration of Mantle Peridotite in the Weathering Horizon. *J. Geophys. Res. Solid Earth* **126**, 1–52 (2021).
65. Oremland, R. S., Whiticar, M. J., Strohmaier, F. E. & Kiene, R. P. Bacterial ethane formation from reduced, ethylated sulfur compounds in anoxic sediments. *Geochim. Cosmochim. Acta* **52**, 1895–1904 (1988).
66. Hinrichs, K.-U. et al. Biological formation of ethane and propane in the deep marine subsurface. *Proc. Natl. Acad. Sci.* **103**, 14684–14689 (2006).
67. Sherwood Lollar, B. et al. Isotopic signatures of CH4 and higher hydrocarbon gases from Precambrian Shield sites: A model for abiogenic polymerization of hydrocarbons. *Geochim. Cosmochim. Acta* **72**, 4778–4795 (2008).
68. McCollom, T. M. Laboratory Simulations of Abiotic Hydrocarbon Formation in Earth's Deep Subsurface. *Rev. Mineral. Geochem.* **75**, 467–494 (2013).
69. Etiope, G. et al. Widespread abiotic methane in chromitites. *Sci. Rep.* **8**, 8728 (2018).
70. Thieringer, P. H., Boyd, E. S., Templeton, A. S. & Spear, J. R. Metapangenomic investigation provides insight into niche differentiation of methanogenic populations from the subsurface serpentinizing environment, Samail Ophiolite, Oman. *Front. Microbiol.* **14**, (2023).
71. Lods, G., Roubinet, D., Matter, J. M., Leprovost, R. & Gouze, P. Groundwater flow characterization of an ophiolitic hard-rock aquifer from cross-borehole multi-level hydraulic experiments. *J. Hydrol.* **589**, 125152 (2020).
72. Paukert, A. Mineral Carbonation in Mantle Peridotite of the Samail Ophiolite , Oman : Implications for permanent geological carbon dioxide capture and storage. (Columbia University2014).
73. Ternieten, L., Fruh-Green, G. L. & Bernasconi, S. M. Carbon Geochemistry of the Active Serpentinization Site at the Wadi Tayin Massif: Insights From the ICDP Oman Drilling Project: Phase II. *J. Geophys. Res. Solid Earth* **126**, (2021).
74. Paukert Vankeuren, A. N., Matter, J. M., Stute, M. & Kelemen, P. B. Multitracer determination of apparent groundwater ages in peridotite aquifers within the Samail ophiolite, Sultanate of Oman. *Earth Planet. Sci. Lett.* **516**, 37–48 (2019).
75. Paukert Vankeuren, A. N. et al. Young apparent ages (<1000 years) of hyperalkaline groundwater in the peridotite section of the Samail Ophiolite, Oman ORAL PRESENTATION. in (Goldschmidt Conference, Lyon, France, 2023).
76. Howells, A. E. G. et al. Energetically Informed Niche Models of Hydrogenotrophs Detected in Sediments of Serpentinized Fluids of the Samail Ophiolite of Oman. *J. Geophys. Res. Biogeosciences* **127**, e2021JG006317 (2022).
77. Canovas, P. A., Hoehler, T. & Shock, E. L. Geochemical bioenergetics during low-temperature serpentinization: An example from the Samail ophiolite, Sultanate of Oman. *J. Geophys. Res. Biogeosci.* **122**, 1821–1847 (2017).
78. Boulart, C. et al. Differences in gas venting from ultramafic-hosted warm springs : the example of Oman and Voltri Ophiolites. *Ofioliti* **38**, 143–156 (2013).
79. Proskurowski, G., Lilley, M. D., Kelley, D. S. & Olson, E. J. Low temperature volatile production at the Lost City Hydrothermal Field, evidence from a hydrogen stable isotope geothermometer. *Chem. Geol.* **229**, 331–343 (2006).
80. Aquino, K. A. et al. Multi-stage evolution of the Lost City hydrothermal vent fluids. *Geochim. Cosmochim. Acta* **332**, 239–262 (2022).
81. Bradley, A. S. & Summons, R. E. Multiple origins of methane at the Lost City Hydrothermal Field. *Earth Planet. Sci. Lett.* **297**, 34–41 (2010).
82. Lang, S. Q. et al. Deeply-sourced formate fuels sulfate reducers but not methanogens at Lost City hydrothermal field. *Sci. Rep.* **8**, 1–10 (2018).
83. Matter, J. M. et al. Oman Drilling Project Phase I Borehole Geophysical Survey. in vol. 2017 V43G-2950 (2017).
84. Takai, K. et al. Cell proliferation at 122 C and isotopically heavy CH4 production by a hyperthermophilic methanogen under high-pressure cultivation. *Proc. Natl. Acad. Sci.* **105**, 10949–10954 (2008).
85. Osselin, F. et al. Orange hydrogen is the new green. *Nat. Geosci.* **15**, 765–769 (2022).
86. Lowe, D. C., Brenninkmeijer, C. A. M., Tyler, S. C. & Dlugkencky, E. J. Determination of the isotopic composition of atmospheric methane and its application in the Antarctic. *J. Geophys. Res. Atmospheres* **96**, 15455–15467 (1991).
87. Petrenko, V. V. et al. A New Method for Analyzing 14C of Methane in Ancient Air Extracted from Glacial Ice. *Radiocarbon* **50**, 53–73 (2008).
88. Nothaft, D. Dissolved inorganic carbon concentration and 13C/12C. (2019) https://doi.org/10.17504/protocols.io.zduf26w.
89. Nothaft, D. B. Bubble strip aqueous gas sampling. https://www.protocols.io/view/bubble-strip-aqueous-gas-sampling-bkb9ksr6 (2020).
90. Hamilton, T. L., Peters, J. W., Skidmore, M. L. & Boyd, E. S. Molecular evidence for an active endogenous microbiome beneath glacial ice. *ISME J.* **7**, 1402–1412 (2013).
91. Weinstein, M. M., Prem, A., Jin, M., Tang, S. & Bhasin, J. M. FIGARO: An efficient and objective tool for optimizing microbiome rRNA gene trimming parameters. *bioRxiv* (2019) https://doi.org/10.1101/610394.
92. Callahan, B. J. et al. DADA2: High-resolution sample inference from Illumina amplicon data. *Nat. Methods* **13**, 581–583 (2016).

93. Wang, Q., Garrity, G. M., Tiedje, J. M. & Cole, J. R. Naive Bayesian classifier for rapid assignment of rRNA sequences into the new bacterial taxonomy. *Appl. Environ. Microbiol.* **73**, 5261–5267 (2007).
94. Quast, C. et al. The SILVA ribosomal RNA gene database project: improved data processing and web-based tools. *Nucleic Acids Res.* **41**, D590–D596 (2013).
95. Nothaft, D. B. danote/Samail_16S_compilation: Second release of Samail 16S data processing repository. Zenodo https://doi.org/10.5281/zenodo.17594721 (2025).

Acknowledgements
This work was supported by the collective contributions of The Oman Drilling Project Science Team. We thank the Ministry of Regional Municipalities and Water Resources in the Sultanate of Oman (particularly Said Al Habsi, Rashid Al Abri, Salim Al Khanbashi, and Haider Ahmed Mohammed Alajmi) for allowing access to wells and logistical support, Zaher Al Sulaimani and Mazin Al Sulaimani from the Oman Water Centre and AZD Engineering for their technical and logistical support, the INSTAAR Laboratory for AMS Radiocarbon Preparation and Research (Scott Lehman, Chad Wolak, and Steve Morgan) and Stratum Reservoir (Isotech) for assisting with radiocarbon sample preparation and analysis.

Author contributions
D.B.N. contributed conceptualization, investigation, metholodogy, data curation, visualization, and writing of the original draft and reviewing and editing. A.S.T., E.S.B., J.M.M., and P.B.K. contributed conceptualization, investigation, funding acquisition, project administration, supervision, and reviewing and editing.

Funding
This research was directly supported by the Rock-Powered Life NASA Astrobiology Institute (NNA15BB02A). This research also used samples and/or data provided by the Oman Drilling Project. The Oman Drilling Project (OmanDP) has been possible through co-mingled funds from the International Continental Scientific Drilling Project (ICDP), the Sloan Foundation–Deep Carbon Observatory (Grant 2014-3-01, Kelemen PI), the National Science Foundation (NSF-EAR-1516300, Kelemen PI), the NASA Astrobiology Institute (NNA15BB02A), the German Research Foundation (DFG), the Japanese Society for the Promotion of Science (JSPS), the European Research Council, the Swiss National Science Foundation, JAMSTEC, the TAMU-JR Science operator, and contributions from the Sultanate of Oman Ministry of Regional Municipalities and Water Resources, the Oman Public Authority of Mining, Sultan Qaboos University, CNRS-Univ. Montpellier II, Columbia University, and the University of Southampton. Publication of this article was funded by the University of Colorado Boulder Libraries Open Access Fund.

Declarations

Competing interests
D.B.N. is CEO of Uplift Geosystems LLC, a company involved in metallurgical and carbon removal technologies. A.S.T. is a minor shareholder in Eden GeoPower, Inc., a reservoir stimulation company with applications in the geothermal, mining, and petroleum industries. J.M.M. is Chief Scientific Officer of Protostar Group Ltd DBA 44.01, a company that stores CO2 in peridotites. P.B.K. is a minor shareholder in Heirloom Carbon Technologies, Inc., a CO2 direct air capture company. P.B.K., J.M.M., and Columbia University hold US Patent 8524152, 'Systems and methods for enhancing rates of in situ carbonation in peridotite'. E.S.B. has no competing interests to declare.

Additional information
Supplementary Information The online version contains supplementary material available at https://doi.org/10.1038/s41598-025-34170-5.

Correspondence and requests for materials should be addressed to D.B.N. or A.S.T.

Reprints and permissions information is available at www.nature.com/reprints.

Publisher's note Springer Nature remains neutral with regard to jurisdictional claims in published maps and institutional affiliations.

Open Access This article is licensed under a Creative Commons Attribution 4.0 International License, which permits use, sharing, adaptation, distribution and reproduction in any medium or format, as long as you give appropriate credit to the original author(s) and the source, provide a link to the Creative Commons licence, and indicate if changes were made. The images or other third party material in this article are included in the article's Creative Commons licence, unless indicated otherwise in a credit line to the material. If material is not included in the article's Creative Commons licence and your intended use is not permitted by statutory regulation or exceeds the permitted use, you will need to obtain permission directly from the copyright holder. To view a copy of this licence, visit http://creativecommons.org/licenses/by/4.0/.

© The Author(s) 2025, corrected publication 2026